Molecular Pharmacology Fast Forward. Published on February 24, 2014 as doi:10.1124/mol.113.089805
This article has not been copyedited and formatted. The final version may differ from this version.

Renal circadian clock regulates the dosing-time dependency of cisplatin-induced nephrotoxicity in mice

Masayuki Oda, Satoru Koyanagi, Yuuya Tsurudome, Takumi Kanemitsu,

Naoya Matsunaga, and Shigehiro Ohdo

Department of Pharmaceutics, Graduate School of Pharmaceutical Sciences,

Kyushu University, 3-1-1 Maidashi Higashi-ku, Fukuoka 812-8582, Japan

Molecular Pharmacology Fast Forward. Published on February 24, 2014 as DOI: 10.1124/mol.113.089805
This article has not been copyedited and formatted. The final version may differ from this version.

Running title:

Circadian regulation of cisplatin-induced nephrotoxicity

Correspondence:

Shigehiro Ohdo, Ph.D., Department of Pharmaceutics, Graduate School of Pharmaceutical Sciences, Kyushu University,

3-1-1 Maidashi Higashi-ku, Fukuoka 812-8582, Japan.

Tel.: 81-92-642-6610; Fax: 81-92-642-6614; E-mail: ohdo@phar.kyushu-u.ac.jp

Document information:

Number of text pages, 34

Number of figures, 7

Number of references, 46

Number of words in the Abstract, 220

Number of words in the Introduction, 738

Number of words in the Discussion, 1026

Abbreviations: BUN, blood urea nitrogen; CDDP, *cis*-diamminedichloro-platinum(II); CLr, renal clearance; GFR, glomerular filtration rate; MATE1, multidrug and toxin extrusion 1; OCT2, organic cation transporter 2

Molecular Pharmacology Fast Forward. Published on February 24, 2014 as DOI: 10.1124/mol.113.089805
This article has not been copyedited and formatted. The final version may differ from this version.

Abstract

Cisplatin, *cis*-diamminedichloro-platinum (CDDP), is a widely used anticancer agent, the clinical applications of which have been limited by severe nephrotoxicity. Although dosing time-dependent differences in CDDP-induced nephrotoxicity have been reported in both humans and laboratory animals, the underlying mechanism remains unknown. In the present study, we investigated the molecular mechanism for the dosing time-dependency of the nephrotoxic effect of CDDP in mice. CDDP-induced nephrotoxicity was significantly attenuated by injecting CDDP at times of the day when its renal clearance was enhanced. The dosing time-dependency of the nephrotoxic effect was parallel to that of CDDP incorporation into renal DNA. Two types of transporters, organic cation transporter 2 (OCT2, encoded by *Slc22a2*) and multidrug and toxin extrusion 1 (MATE1, encoded by *Slc47a1*), are responsible for the renal excretion of CDDP. The expression of OCT2, but not MATE1, exhibited a significant time-dependent oscillation in the kidneys of mice. The circadian expression of OCT2 was closely related to the dosing time-dependency of CDDP incorporation into renal DNA. Molecular components of the circadian clock regulated the renal expression of *Slc22a2* mRNA by mediating peroxisome proliferator activated receptor α (PPARα), which resulted in rhythmic oscillations in OCT2 protein levels. These findings indicate a clock-regulated mechanism of dosing time-dependent changes in CDDP-induced nephrotoxicity and also suggest a molecular link between the circadian clock and renal xenobiotic excretion.

Molecular Pharmacology Fast Forward. Published on February 24, 2014 as DOI: 10.1124/mol.113.089805
This article has not been copyedited and formatted. The final version may differ from this version.

Introduction

Daily variations in biological functions such as gene expression and protein synthesis are thought to be important factors affecting the efficacy of drugs. Dosing time-dependent differences in the therapeutic effects of drugs are, at least in part, due to circadian-related changes in drug disposition such as absorption, distribution, metabolism, and elimination (Labrecque and Bélanger, 1991; Bélanger et al., 1997; Ohdo, 2007, 2010). In mammals, the master circadian pacemaker resides in the suprachiasmatic nucleus of the anterior hypothalamus, and is responsible for adapting endogenous physiological functions to daily environmental cues such as light and food (Green et al., 2008; Bass and Takahashi, 2010; Asher and Schibler, 2011; Morf et al., 2012). The mammalian circadian clock constitutes a transcriptional-translational feedback loop, in which CLOCK and BMAL1 activate the transcription of *Period* (*Per*) and *Cryptochrome* (*Cry*) via E-box enhancer sequences (Green et al., 2008; Bass and Takahashi, 2010; Asher and Schibler, 2011). Once PER and CRY proteins have reached critical concentrations, they attenuate CLOCK/BMAL1 transactivation, thereby generating circadian oscillations in their own transcription. The transcription of orphan nuclear receptor *Rev-erbα* and *activating transcription factor-4* (*Atf4*) are also activated by CLOCK/BMAL1 and repressed by PER and CRY, resulting in circadian oscillations in the transcription of *Bmal1* (Preitner et al., 2002; Koyanagi et al., 2011).

The molecular oscillator regulates daily variations in output physiology through clock-controlled output genes (Jin et al., 1999; Maemura et al., 2000; Cheng et al., 2002). Proline- and acid-rich (PAR) basic leucine zipper (bZIP) proteins, hepatic leukemia factor

Molecular Pharmacology Fast Forward. Published on February 24, 2014 as DOI: 10.1124/mol.113.089805
This article has not been copyedited and formatted. The final version may differ from this version.

(HLF), thyrotroph embryonic factor (TEF), and D-site binding protein (DBP) are examples of such output mediators, because their expression is probably regulated by core oscillator components (Gachon et al., 2004). Circadian-controlled output pathways include xenobiotic detoxification mediated through the circadian expression of many enzymes and transporters. (Gachon et al., 2006). Clock genes comprising the core oscillation loop have also been shown to govern the expression of peroxisome proliferator-activated receptor-α (PPARα) (Oishi et al., 2005). PPARα controls the transcription of its target genes through PPAR response elements (PPREs) and participates in the circadian expression of fibroblast growth factor-21 and plasminogen activator inhibitor-1 (Oishi et al., 2008). Recent studies have revealed that PPARα regulates the transcription of several types of transporters, including fatty acid transport protein (FATP), ATP-binding cassette-transporter family A1 (ABCA1), and equilibrative nucleoside transporter 1 (ENT1) (Martin et al., 1997; Chinetti et al., 2001; Montero et al., 2012), suggesting that the function and expression of PPARα-targeted transporters may also exhibit circadian oscillations.

Cisplatin, *cis*-diamminedichloro-platinum (CDDP), is a platinum (Pt)-based anticancer agent that is widely used in the treatment of solid cancers, such as lung, ovarian, and esophageal cancers. However, CDDP can cause severe nephrotoxicity, which is a dose-limiting factor of CDDP therapy. Recent studies have reported that organic cation transporter 2 (OCT2) and multidrug and toxin extrusion 1 (MATE1) are responsible for CDDP-induced nephrotoxicity (Filipski et al., 2009; Nakamura et al., 2010). OCT2 is expressed in the basolateral membrane of proximal tubule cells in the kidney, whereas MATE1 is located in the brush border membrane. CDDP is incorporated into renal cells by

Molecular Pharmacology Fast Forward. Published on February 24, 2014 as DOI: 10.1124/mol.113.089805
This article has not been copyedited and formatted. The final version may differ from this version.

OCT2, and then MATE1 excretes this drug into the urine. The incorporated CDDP in cells forms DNA adducts and activates apoptotic signals, resulting in renal cell death. Therefore, much effort has been directed toward attenuating CDDP-induced nephrotoxicity (Pabla and Dong, 2008; Miller et al., 2010; dos Santos et al., 2012). For example, hydration with sodium chloride is frequently given before and/or during CDDP therapy to prevent its accumulation in renal cells. A previous study showed that hydration decreased CDDP-induced nephrotoxicity by 60-70% in rats (Litterst, 1981)

On the other hand, a significant dosing time-dependent difference in CDDP-induced nephrotoxicity has been reported in both humans and laboratory animals (Levi et al., 1982a; 1982b; Hrushesky et al., 1982; Boughattas et al., 1990). CDDP-induced nephrotoxicity was attenuated in humans by administering the drug during the afternoon. Consequently, CDDP has been empirically administered to patients during these time windows. However, the mechanism underlying dosing time-dependent changes in CDDP-induced nephrotoxicity remain to be clarified.

In this study, we investigated the mechanism underlying dosing time-dependent differences in CDDP-induced nephrotoxicity in mice. CDDP-induced nephrotoxicity varied according to circadian changes in the renal excretion function. CDDP-induced nephrotoxicity was attenuated by injecting CDDP at times of the day when renal CDDP clearance was increased. Therefore, we focused on the function of OCT2 and MATE1 to investigate the underlying mechanism of dosing time-dependent changes in CDDP-induced nephrotoxicity.

Molecular Pharmacology Fast Forward. Published on February 24, 2014 as DOI: 10.1124/mol.113.089805
This article has not been copyedited and formatted. The final version may differ from this version.

Materials and methods

Animals and cells. Male *Clock* mutant (*Clock/Clock*) mice (C57BL/6J*Clock*$^{m1Jt/J}$) on a ICR background, male PPARα-null mice (crossed 129S4SvJae- PPARα^{tm1Gonz}/J with Jcl:ICR), and male wild-type mice of the same strain were kept in a temperature-controlled room (24 ± 1 °C) under a 12-h light: 12-h dark cycle with food and water *ad libitum*. Under the light/dark cycle, Zeitgeber time (ZT) 0 was designated as lights on and ZT12 as lights off. Animals were cared for in accordance with the guidelines established by the Animal Care and Use Committee of Kyushu University.

NIH3T3 cells were supplied by the Cell Resource Center for Biomedical Research, Tohoku University (Sendai, Japan). NIH3T3 cells were maintained in Dulbecco's Modified Eagle Medium (DMEM) (Sigma-Aldrich, St. Louis, MO) supplemented with 10% FBS (AFC Biosciences, Lenexa, KS) at 37 °C under a humidified 5% CO_2 atmosphere.

Determination of blood urea nitrogen (BUN) levels. Mice were injected intravenously with a single dose of 15 mg/kg CDDP (Wako, Osaka, Japan) or equivalent volume of saline at ZT2, ZT6, ZT10, ZT14, ZT18, or ZT22, and blood samples were collected 72 h after the injection. Serum was separated by centrifugation. Serum BUN levels were determined using a manufactured kit (Wako Chemical Industry, Osaka, Japan).

Pharmacokinetic analysis of CDDP. To estimate dosing time-dependent differences in the pharmacokinetic parameters of CDDP, mice were injected intravenously with a single dose of 15 mg/kg CDDP at ZT2 and ZT14. During the duration of

Molecular Pharmacology Fast Forward. Published on February 24, 2014 as DOI: 10.1124/mol.113.089805
This article has not been copyedited and formatted. The final version may differ from this version.

experiment, mice were kept individually in cages containing paper bedding (Oriental Yeast Co., Ltd., Tokyo, Japan). Blood samples were drawn via the orbital sinus 1 h and 4 h after the CDDP injection. At the same time, urinary volume was measured by calculating differences in the weight of paper bedding before and after the experiment. The loss of evaporated urine from paper bedding during the duration of the experiment was adjusted for by measuring the evaporation loss of 2.0 mL water from the bedding. Platinum (Pt) concentrations in the serum and urine were determined by inductively coupled plasma mass spectrometry (ICP-MS). The area under the serum Pt concentration-time curve from 1 h to 4 h after the CDDP injection ($AUC_{1\text{-}4}$) was calculated according to the trapezium rule. The renal clearance (CLr) of CDDP during the elimination phase was calculated using the following equation: $CLr = U \times ke / (C_1 - C_4)$, where U is the total amount of urinary Pt excretion; ke is the elimination rate constant; C_1 and C_4 are serum Pt concentrations 1 h and 4 h after the CDDP injection, respectively.

Determination of Pt incorporation into renal DNA. After obtaining blood and urine samples for pharmacokinetic analysis, the kidneys were removed from mice to determine the amount of Pt incorporated into renal DNA. Genomic DNA was extracted from the renal cortex using the Wizard Genomic DNA Purification Kit (Promega, San Luis Obispo, CA). Pt concentrations were measured in renal genomic DNA by ICP-MS as described above, and Pt incorporation into renal DNA was expressed as the Pt amount (pg) per μg of DNA.

Determination of the glomerular filtration rate. The glomerular filtration rate (GFR) was determined by estimating the renal clearance of fluorescein isothiocyanate

Molecular Pharmacology Fast Forward. Published on February 24, 2014 as DOI: 10.1124/mol.113.089805
This article has not been copyedited and formatted. The final version may differ from this version.

(FITC)-inulin (Sigma-Aldrich, St. Louis, MO), as described previously (Qi et al., 2004). To remove residual FITC not bound to inulin, FITC-inulin powder was dissolved in saline and dialyzed at room temperature for 24 h using a 1000-Da cutoff dialysis membrane (Tube-O-DIALYZER, Wako, Osaka, Japan). FITC-inulin was continuously infused into mice using an osmotic minipump (Model 1007D, ALZET, Cupertino, CA). A micro-osmotic pump filled with 100 μL of dialyzed 5% FITC-inulin was implanted into the dorsal skin of mice. Mice were transferred into individual cages containing paper bedding. Six days after implantation, blood samples were drawn via the orbital sinus at ZT4 and ZT16. Urine volumes during ZT2-6 or ZT14-18 were measured on the same day, as described above. FITC-inulin concentrations in the serum and urine were determined by spectrofluorometry. Renal clearance of FITC-inulin (GFR) was calculated by the following equation: GFR = U / Css; where U is the total amount of urinary excreted FITC-inulin per 1 h; Css is the serum FITC-inulin concentration at a steady-state.

Western blot analysis. To extract renal membrane fractions, the kidneys were homogenized with Krebs-Ringer buffer (11.7 mM NaCl, 4.7 mM KCl, 1.2 mM $MgCl_2$, 1.2 mM $NaH_2PO_4 \cdot 2H_2O$, 25 mM $NaHCO_3$, 2.5 mM $CaCl_2 \cdot 2H_2O$, 11 mM D-(+)-glucose). Whole lysate was separated by centrifugation for 15 min at 8 000 × g, 4 °C, and the resulting supernatant was ultracentrifuged at 100,000 × g, 4 °C for 1 h. The obtained pellet was resuspended in 20 mM Mops-Tris, pH. 7.0, 300 mM sucrose, 5 mM EDTA, protease inhibitor (2 μg/mL leupeptin, 2 μg/mL aprotinin and 100 μM PMSF), and was further ultracentrifuged at 100,000 × g, 4 °C for 1 h. The pellet was resuspended in Tris-EDTA buffer (10 mM Tris-HCl, 5mM EDTA, pH7.0) containing appropriate protease

Molecular Pharmacology Fast Forward. Published on February 24, 2014 as DOI: 10.1124/mol.113.089805
This article has not been copyedited and formatted. The final version may differ from this version.

inhibitors. This suspension was used as the renal membrane fraction. Renal nuclear fractions were prepared using an NE-PER extraction kit (Pierce Biotechnology, Inc., Rockford, IL, USA). Renal membrane fractions were denatured at 60 °C for 30 min with 0.1% TritonX-100, 1% SDS, and 5% 2-mercaptethanol, while renal nuclear fractions were denatured at 99 ℃ for 5 min with 1% SDS, and 5% 2-mercaptethanol. Denatured renal membrane or nuclear fraction samples were separated by SDS-PAGE. Separated proteins were transferred to a polyvinylidene difluoride membrane and reacted against OCT2 (Alpha Diagnostic International, San Antonio, Texas), MATE1 (kindly provided by Dr. M. Otsuka, Setsunan University, Osaka, Japan), TATA-binding protein (TBP; Abcam, Cambridge, England), and PPARα and RXRα (Santa Cruz Biotechnology, Santa Cruz, CA) antibodies. Specific antigen-antibody complexes were visualized using horseradish peroxidase-conjugated secondary antibodies and Chemi-Lumi One (Nacalai Tesque Inc., Kyoto, Japan) or Immuno Star LD (Wako, Osaka, Japan). Visualized images were scanned by LAS4000.

Quantitative RT-PCR analysis. Total RNA was extracted using RNAiso reagent (Takara Co., Ltd., Osaka, Japan). Complementary DNA (cDNA) was synthesized by reverse-transcribing 1 μg of RNA using a ReverTra Ace qPCR RT kit (Toyobo, Osaka, Japan). The cDNA equivalent of 10 ng of RNA was amplified by PCR in a real-time PCR system (Applied Biosystems, Life Technologies, Carlsbad, CA, USA). Sequences for PCR primers are described as follows: *Slc22a2*, 5'-AGCCTGCCTAGCTTCGG -TTT-3' and 5'-TGCCCATTCTACCCAAGCA-3'; *Slc47a1*, 5'-AGGCCAAGAAGTCCTCAG -CTATT-3' and 5'-ACGCAGAAGGTCACAGCAAA-3'; *β-Actin*, 5'-CACA

Molecular Pharmacology Fast Forward. Published on February 24, 2014 as DOI: 10.1124/mol.113.089805
This article has not been copyedited and formatted. The final version may differ from this version.

-CCTTCTACAATGAGCTGC-3' and 5'-CATGATCTGGGTCATCTTTTCA-3'.

Construction of reporter and expression vectors. The mouse *Slc22a2* promoter region spanning from bp -2101 to +20, -1331 to +20, and -482 to +20 (relative to the transcription start site, +1) was amplified by PCR, and the products were ligated into the pGL4.12 luciferase reporter vector (Promega, San Luis Obispo, CA). Expression vectors for mouse PPARα, RXRα, RORα, and ATF4 were constructed using cDNA generated from mouse liver RNA by RT-PCR. All coding regions were ligated into the pcDNA3.1(+) vector (Invitrogen, Carlsbad, CA)

Luciferase reporter assays. NIH3T3 cells were seeded at a density of 3×10^4/well in 24-well culture plates. Cells were transfected with 25 ng of the pGL4.12 reporter construct and 1 μg (total) of expression vectors. The pcDNA3.1 empty vector was added to adjust the total amount of DNA in all transfections. A total of 10 pg of the pRL-SV40 vector (Promega, San Luis Obispo, CA) was also transfected as an internal control reporter. To transfect the ATF4 expression vector, cells were incubated in DMEM supplemented with 2% FBS during the transfection to minimize the effects of FBS on activating CRE-mediated signaling. Cells were harvested 24 h after transfection, and the lysates were analyzed using a Dual-Luciferase reporter assay system (Promega, San Luis Obispo, CA). The ratio of firefly (expressed from the pGL4.12 reporter construct) to Renilla (expressed from pRL-SV40) luciferase activities in each sample served as a measure of normalized luciferase activity.

Chromatin immunoprecipitation (ChIP) analysis. Crosslinked chromatin from the

Molecular Pharmacology Fast Forward. Published on February 24, 2014 as DOI: 10.1124/mol.113.089805
This article has not been copyedited and formatted. The final version may differ from this version.

kidney was sonicated on ice, and nuclear fractions were obtained by centrifugation at 13,000 × g for 10 min. Supernatants were incubated with antibodies against PPARα (Santa Cruz Biotechnology, Santa Cruz, CA) coupled to Dynabeads protein G (Invitrogen, Carlsbad, CA) using bis(sulfosuccinimidyl) suberate cross-linker according to the manufacturer's instructions. DNA was isolated from immunoprecipitants and then amplified by PCR for the surrounding PPREs in the 5'-flanking region of *Slc22a2* genes (from bp -1942 to -1774) using following primer pairs; 5'-TGATCAATG -TCCCAGATGACCCTCA-3' and 5'-AGGTGAGCAGGCAGCTAGCTC-3'. The quantitative reliability of PCR was evaluated by kinetic analysis of the amplified products to ensure that signals were derived only from the exponential phase of amplification. ChIP proceeded in the presence of rabbit IgG as negative controls.

Simulation of CDDP accumulation into renal DNA. We hypothesized that CDDP would be incorporated into renal cells at a constant rate (k_{in}, influx rate constant) and excreted in the urine at a first order rate (k_{out}, efflux rate constant). To assess an *in vivo* simulation, the average of OCT2 or MATE1 protein band intensities at ZT2 and ZT6 was expressed as k_{in} or k_{out} during the light phase, and the average at ZT14 and ZT18 was expressed during the dark phase, respectively. The volume of CDDP distribution in renal cells (*Vc*) was fitted to the actual values of Pt incorporation into renal DNA in Figure 2B because we were unable to estimate *Vc* in renal DNA.

Statistical analysis. The significance of the 24-h variation in each parameter was tested by an analysis of variance (ANOVA). The significance of differences among groups was analyzed by ANOVA and the Tukey-Kramer post hoc test. A paired *t* test was

Molecular Pharmacology Fast Forward. Published on February 24, 2014 as DOI: 10.1124/mol.113.089805
This article has not been copyedited and formatted. The final version may differ from this version.

used for comparison analysis within the same group, and an unpaired *t* test for the comparison of data between two groups. A 5% level of probability was considered to be significant.

Results

Dosing-time dependency of CDDP-induced nephrotoxicity in mice. To test whether CDDP-induced nephrotoxicity changed depending on its dosing time, mice were injected with a single intravenous dosage of CDDP (15 mg/kg) at 6 different time points. At 72 h after the CDDP injection, serum BUN levels in wild-type mice were elevated in a dosing time-dependent manner (**Fig. 1A**). Serum BUN levels were significantly increased after the CDDP injection at ZT6 ($P<0.05$); a significant elevation in BUN levels was not observed when mice were injected with CDDP at the other dosing times. In contrast, no significant dosing time-dependent differences were observed in serum BUN levels after the CDDP injection in *Clock/Clock* mice (**Fig. 1B**). Serum BUN levels in *Clock/Clock* mice were elevated after the CDDP injection at both dosing times, ZT6 and ZT18. These results indicate that CDDP-induced nephrotoxicity in wild-type mice could be attenuated by changing the dosing time. Dosing time-dependent differences in CDDP-induced nephrotoxicity appear to be under the control of the molecular clockwork.

Dosing-time dependency of CDDP pharmacokinetics in mice. To elucidate the underlying mechanism of the dosing time-dependency of CDDP-induced nephrotoxicity, we performed pharmacokinetic analysis of CDDP in wild-type and *Clock/Clock* mice after injecting the drug at ZT2 and ZT14. The area under the curve ($AUC_{1\text{-}4}$) of serum Pt

Molecular Pharmacology Fast Forward. Published on February 24, 2014 as DOI: 10.1124/mol.113.089805
This article has not been copyedited and formatted. The final version may differ from this version.

concentrations following the CDDP injection in wild-type mice at ZT14 was significantly lower than that at ZT2 ($p<0.05$, **Fig. 2A**). Although significant dosing time-dependent differences were also observed in $AUC_{1\text{-}4}$ after the CDDP injection in *Clock/Clock* mice, $AUC_{1\text{-}4}$ values in *Clock/Clock* mice were higher than those in wild-type mice (**Fig. 2A**).

CDDP is mainly excreted from the kidney (Lange et al., 1972; Siddik et al., 1987). Since CDDP is retained in the renal tissue for a long period of time, it may readily cause nephrotoxicity (Farris et al., 1988). The renal clearance of CDDP after its injection in wild-type mice varied in a dosing time-dependent manner (**Fig. 2B**). The renal clearance of CDDP in wild-type mice after its injection at ZT14 was significantly higher than that at ZT2 ($p<0.05$). On the other hand, no significant difference in the renal clearance of CDDP was observed in *Clock/Clock* mice. The renal clearance of CDDP in *Clock/Clock* mice was low at both dosing times.

Consistent with these results, dosing time-dependent differences were also observed in Pt incorporation into the renal DNA of wild-type mice (**Fig. 2C**). The incorporation of Pt into renal DNA after the CDDP injection at ZT14 tended to be lower than that at ZT2. On the other hand, no significant dosing time-dependent differences were observed in Pt incorporation into the renal DNA of *Clock/Clock* mice (**Fig. 2C**). The amount of incorporated Pt in the renal DNA of *Clock/Clock* mice was higher than that of wild-type mice. These results indicate that the dosing-time dependency of CDDP-induced nephrotoxicity can be attributed to circadian variations in renal excretion function. The kidney may be exposed to high concentrations of CDDP after its injection at times of the day when renal excretion function is decreased. Because *Clock/Clock* mice failed to show

Molecular Pharmacology Fast Forward. Published on February 24, 2014 as DOI: 10.1124/mol.113.089805
This article has not been copyedited and formatted. The final version may differ from this version.

a significant dosing time-dependency in CDDP pharmacokinetics, the renal function for xenobiotic excretion appears to be under the control of the molecular clockwork.

The renal clearance of CDDP consists of both glomerular filtration and transporter-mediated tubular secretion. The GFR of wild-type mice exhibited significant time-dependent variations ($p<0.05$, **Fig. 2D**), with the filtration rate being facilitated during the dark phase. This may also contribute to dosing time-dependent differences in the renal clearance of CDDP. On the other hand, GFR did not show significant time-dependent variations in *Clock/Clock* mice; the contribution rate of GFR to renal clearance of CDDP was over 60 % at both light and dark phases. Conversely, these results suggest that tubular secretion clearance of CDDP is reduced in *Clock/Clock* mice.

Circadian oscillations in the renal expression of OCT2. In the kidney, CDDP is taken up into the renal proximal tubular cells mainly via *Slc22a2* organic cation transporter 2 (OCT2) and is secreted into the lumen via other transporters including the *Slc47a1* multidrug and toxin extrusion 1 (MATE1) (Filipski et al., 2009; Nakamura et al., 2010; Yonezawa et al., 2006). The levels of *Slc22a2* mRNA and OCT2 protein in the kidneys of wild-type mice showed circadian oscillations (**Fig. 3A**), with these levels being higher around the mid light phase. In contrast, OCT2 protein levels in the kidneys of *Clock/Clock* mice did not show any clear circadian oscillations; the transporter proteins remained at low levels throughout the day. Similar decreases in the amplitude of the *Slc22a2* mRNA oscillation were also observed in the kidneys of *Clock/Clock* mice (**Fig. 3B**), suggesting that the CLOCK protein positively regulates OCT2 expression at the transcriptional level.

Molecular Pharmacology Fast Forward. Published on February 24, 2014 as DOI: 10.1124/mol.113.089805
This article has not been copyedited and formatted. The final version may differ from this version.

The protein levels of MATE1 in the kidneys of wild-type mice failed to show any clear circadian oscillations (**Fig. 3A**), which appeared to be the result of no time-dependent variations in *Slc47a1* mRNA levels (**Fig. 3B**). No clear circadian oscillations in the expression of MATE1 were also found in the kidneys of *Clock/Clock* mice (**Fig. 3A**); the transporter proteins remained at low levels throughout the day. Consequently, *Slc47a1* mRNA levels in *Clock/Clock* mice were significantly lower than those in wild-type mice (**Fig. 3B**). Taken together, these results suggest that the CLOCK protein acts as a positive regulator of *Slc47a1* gene expression, but does not rhythmically derive its expression.

CLOCK protein regulates the expression of Slc22a2 through the mediation of PPARα. To examine how CLOCK protein rhythmically drives the expression of *Slc22a2*, we searched consensus sequences for response elements to circadian transcriptional factors within the promoter region of the mouse *Slc22a2* gene. Four nucleotide sequences showing homology with PPREs were found within 2.1 kilobases (kb) of the *Slc22a2* gene 5'-flanking region (**Fig. 4A**). Furthermore, three ROR response elements (RORE) and two cAMP binding protein (CREB) response elements (CREs) were also identified in the 5'-flanking region. To study the functional importance of these sequences for expression of the *Slc22a2* gene, we performed a transient transcriptional assay using *Slc22a2* luciferase reporter constructs.

As shown in **figure 4B**, co-transfection of the *Slc22a2* (-2,101)-Luc reporter with PPARα and RXRα resulted in a 10-fold increase in transcriptional activity. Although RORα also enhanced transcription of the *Slc22a2* reporter, these enhancement effects

Molecular Pharmacology Fast Forward. Published on February 24, 2014 as DOI: 10.1124/mol.113.089805
This article has not been copyedited and formatted. The final version may differ from this version.

were weaker than those by PPARα/RXRα. Therefore, we further assessed the ability of PPARα and RXRα to regulate *Slc22a2* transcription. Deleting the sequence of the 5'-flanking region of the *Slc22a2* gene from base pair (bp) -2101 to -1331 caused a marked decrease in the transactivation effect of PPARα/RXRα, by approximately 70% (**Fig. 4C**). The nucleotide sequence located between bp -2101 to -1331 in the *Slc22a2* gene showed homology with the two consensus sequences of PPREs (**Fig. 4A**), suggesting that these sites are responsible for the transcriptional regulation of *Slc22a2* by PPARα/RXRα.

The results of western blot analysis revealed that PPARα, but not RXRα, were time-dependently expressed in the kidneys of wild-type mice (**Fig. 5A**). The amount of PPARα in wild-type kidneys increased at the peak time of *Slc22a2* mRNA expression (**Fig. 3A**; see ZT6). In contrast, neither PPARα nor RXRα proteins showed clear time-dependent variations in the kidneys of *Clock/Clock* mice (**Fig. 5A**). PPARα protein levels decreased in *Clock/Clock* mice. In fact, PPARα binding to the promoter region of the mouse *Slc22a2* gene in the kidney of wild-type mice also increased at the times of day when *Slc22a2* mRNA was abundant (**Fig. 5B**), but the time-dependent variation in the PPARα binding was undetectable in *Clock/Clock* mice. Furthermore, the levels of *Slc22a2* mRNA in the kidney of PPARα-null mice failed to show significant time-dependent variation (**Fig. 5C**). These results suggest that the CLOCK-regulated output pathway, including PPARα, contributed to the circadian expression of *Slc22a2* in the kidney. This notion is further supported by the facts that the temporal profiles of renal clearance of CDDP and Pt incorporation into renal DNA of PPARα-null mice exhibited a

Molecular Pharmacology Fast Forward. Published on February 24, 2014 as DOI: 10.1124/mol.113.089805
This article has not been copyedited and formatted. The final version may differ from this version.

similar phenotype as observed in *Clock/Clock* mice (**Fig. 5D and E).**

Discussion

In this study, we used laboratory animals to investigate the mechanism underlying dosing-time dependent differences in CDDP-induced nephrotoxicity from the viewpoint of its pharmacokinetics. Previous studies have suggested that circadian changes in the urinary volume contribute to the dosing time-dependency of CDDP-induced nephrotoxicity because increases in the urinary volume accelerate the excretion of CDDP from the body and prevent the accumulation of Pt in renal cells (Levi et al., 1982b). The renal clearance of CDDP in wild-type mice was significantly increased during the dark phase, such that CDDP-induced nephrotoxicity was attenuated by injecting CDDP at times of the day when renal clearance was enhanced. Therefore, renal cells are more likely to be exposed to high concentrations of CDDP after the drug has been administered during the light phase. In fact, the accumulation of Pt in renal DNA was enhanced by injecting CDDP into wild-type mice during the light phase (ZT6). It is thus possible that the ability of renal cells to uptake CDDP vary in a circadian time-dependent manner.

In renal proximal tubule cells, OCT2 and MATE1 function as key molecules for the excretion of CDDP, and they have been implicated in CDDP-induced nephrotoxicity (Filipski et al., 2009; Nakamura et al., 2010). Mice deficient for both Oct1 and Oct2 were shown to suppress the accumulation of Pt in the kidney following an injection of CDDP (Filipski et al., 2009). Since the expression of OCT2, and not OCT1, is higher at the basolateral site of the renal proximal tubule cells (Urakami et al., 1998; Karbach et al.,

Molecular Pharmacology Fast Forward. Published on February 24, 2014 as DOI: 10.1124/mol.113.089805
This article has not been copyedited and formatted. The final version may differ from this version.

2000; Terada and Inui, 2007), OCT2 appears to promote the incorporation of CDDP into renal cells. On the other hand, mice lacking the *Slc47a1* gene have exhibited severe CDDP-induced nephrotoxicity (Nakamura et al., 2010). Both BUN plasma levels and renal Pt accumulation in CDDP-injected *Slc47a1* knockout mice were significantly higher than those in wild-type mice. Because MATE1, which is encoded by *Slc47a1*, is known to be expressed at the apical site of renal proximal tubule cells (Otsuka et al., 2005), this transporter promotes the excretion of CDDP from renal cells. Although MATE1 protein levels in the kidneys of wild-type mice failed to show clear circadian oscillations, OCT2 protein levels were increased during the light phase. The incorporation of Pt into renal DNA was attenuated by an injection of CDDP during the dark phase. Furthermore, CDDP-induced nephrotoxicity was also significantly attenuated by an injection of CDDP during these time windows. These results suggest that oscillations in the expression of OCT2 in renal proximal tubule cells underlie the dosing time-dependency of CDDP-induced nephrotoxicity (**Fig. 6**). In contrast, *Clock/Clock* mice did not show significant dosing time-dependency of CDDP-induced nephrotoxicity, accompanied by the arrhythmic expression of OCT2 in renal cells. This may account for the importance of the OCT2 expression rhythm in inducing dosing time-dependent changes in CDDP-induced nephrotoxicity. However, despite the low level of OCT2 expression, *Clock/Clock* mice showed severe CDDP-induced nephrotoxicity as well as the higher accumulation of Pt in renal DNA.

To interpret this discrepancy, we focused on differences in MATE1 protein levels between wild-type and *Clock/Clock* mice and attempted a kinetic simulation for Pt

Molecular Pharmacology Fast Forward. Published on February 24, 2014 as DOI: 10.1124/mol.113.089805
This article has not been copyedited and formatted. The final version may differ from this version.

incorporation into renal DNA. The results of the simulation analysis revealed that Pt incorporation into renal DNA was enhanced by decreasing both OCT2 and MATE1 protein levels (**Fig. 7**). Decreases in OCT2 protein levels delayed the incorporation of Pt, whereas low levels of MATE1 expression enhanced the accumulation of Pt in renal cells. Since both OCT2 and MATE1 protein levels were reduced in *Clock/Clock* mice, decreases in the functions of these transporter appeared to enhance the accumulation of Pt in the renal DNA of *Clock/Clock* mice, thereby causing severe CDDP-induced nephrotoxicity at both dosing times (**Fig. 6**).

The CLOCKΔ19 mutant protein, which is produced in *Clock/Clock* mice, can still interact with BMAL1, but fails to activate transcription (Gekakis et al., 1998; Katada et al., 2010); therefore, the amplitude of the rhythm in many circadian genes is reduced in *Clock/Clock* mice. Oscillations in the renal expression of the PPARα protein in wild-type mice corresponded to the rhythm of *Slc22a2* mRNA expression. On the other hand, PPARα protein levels did not show clear time-dependent variations in the kidneys of *Clock/Clock* mice, which suggested that oscillations in the renal expression of the PPARα protein is also under the control of the function of the CLOCK protein. Considering the ability of PPARα to regulate transcription of the *Slc22a2* gene, altered rhythms in the expression of PPARα proteins could account for the blunted rhythm of *Slc22a2* expression in the kidneys of *Clock/Clock* mice. In fact, the time-dependent difference in the PPARα binding to the promoter region of the mouse *Slc22a2* gene was undetectable in the kidney of *Clock/Clock* mice. The blunted rhythm of *Slc22a2* mRNA also appeared to decrease the amplitude of OCT2 oscillations. These results suggest that the CLOCK

Molecular Pharmacology Fast Forward. Published on February 24, 2014 as DOI: 10.1124/mol.113.089805
This article has not been copyedited and formatted. The final version may differ from this version.

protein controls the rhythm of the renal expression of *Slc22a2* mRNA and the OCT2 protein through mediation via PPARα.

PPARα has been shown to function as a nuclear receptor to activate the transcription of its target genes. Previous studies have reported that a number of endogenous substrates, such as polyunsaturated fatty acids, serve as ligand activators of this nuclear receptor (Göttlicher et al., 1992; Keller et al., 1993). Several PPAR agonists were shown to protect against CDDP-induced nephrotoxicity (Li et al., 2003, 2005; Nagothu et al., 2005). The underlying mechanisms were attributed to modulations in the expression of genes such as proinflammatory cytokine tumor necrosis factorα (TNFα), interleukin 6 (IL-6), and proapoptotic Bax (Li et al., 2005; Nagothu et al., 2005). Therefore, the mechanism for the protective actions of PPAR agonists against CDDP-induced nephrotoxicity seems to be distinct from our present findings.

In conclusion, the results of the present study obtained from an animal model suggest a mechanism underlying the dosing time-dependency of CDDP-induced nephrotoxicity and also provide a molecular link connecting the renal circadian clock to renal xenobiotic excretion. Identifying the factors that affect the disposition of drugs is important in order to achieve rational pharmacotherapy in humans. Our present findings may contribute to the optimization of a dosing schedule for CDDP and attenuation of its nephrotoxicity.

Molecular Pharmacology Fast Forward. Published on February 24, 2014 as DOI: 10.1124/mol.113.089805
This article has not been copyedited and formatted. The final version may differ from this version.

Acknowledgments

The authors thank the technical support for measurement of platinum from the Center of Advanced Instrumental Analysis, Kyushu University.

Authorship Contributions

Participated in research design: Oda, Koyanagi, Matusnaga, and Ohdo.

Conducted experiments: Oda, Koyanagi, Tsurudome, and Kanemitsu.

Contributed new reagents or analytic tools: Oda, Tsurudome, and Matusnaga.

Performed data analysis: Oda and Koyanagi.

Wrote or contributed to the writing of the manuscript: Oda, Koyanagi, and Ohdo.

Molecular Pharmacology Fast Forward. Published on February 24, 2014 as DOI: 10.1124/mol.113.089805
This article has not been copyedited and formatted. The final version may differ from this version.

References

Asher G and Schibler U (2011) Crosstalk between Components of Circadian and Metabolic Cycles in Mammals. *Cell Metab* **13:** 125-137.

Bass J and Takahashi JS (2010) Circadian Integration of Metabolism and Energetics. *Science* **330:** 1349-1354.

Bélanger PM, Bruguerolle B, and Labrecque G (1997) Rhythms in Pharmacokinetics: Absorption, Distribution, Metabolism, and Excretion. *Handb Exp Pharmacol* **125:** 177-204.

Boughattas NA, Lévi F, Fournier C, Hecquet B, Lemaigre G, Roulon A, Mathé G, and Reinberg A (1990) Stable circadian mechanisms of toxicity of two platinum analogs (cisplatin and carboplatin) despite repeated dosages in mice. *J Pharmacol Exp Ther* **255:** 672-679.

Cheng MY, Bullock CM, Li C, Lee AG, Bermak JC, Belluzzi J, Weaver DR, Leslie FM, and Zhou QY (2002) Prokineticin 2 transmits the behavioural circadian rhythm of the suprachiasmatic nucleus. *Nature*, **417:** 405-410.

Chinetti G, Lestavel S, Bocher V, Remaley AT, Neve B, Torra IP, Teissier E, Minnich A, Jaye M, Duverger N, Brewer HB, Fruchart JC, Clavey V, and Staels B (2001) PPAR-α and PPAR-γ activators induce cholesterol removal from human macrophage foam cells through stimulation of the ABCA1 pathway. *Nat Med* **7:** 53-58.

dos Santos NA, Carvalho Rodrigues MA, Martins NM, and dos Santos AC (2012) Cisplatin-induced nephrotoxicity and targets of nephroprotection: an update. *Arch Toxicol* **86:** 1233-1250.

Farris FF, Dedrick RL, and King FG (1988) Cisplatin pharmacokinetics: applications of a physiological model. *Toxicol Lett* **43:** 117-137.

Filipski KK, Mathijssen RH, Mikkelsen TS, Schinkel AH, and Sparreboom A (2009) Contribution of Organic Cation Transporter 2 (OCT2) to Cisplatin-Induced Nephrotoxicity. *Clin Pharmacol Ther* **86:** 396-402.

Gachon F, Fonjallaz P, Damiola F, Gos P, Kodama T, Zakany J, Duboule D, Petit B, Tafti M, and Schibler U (2004) The loss of circadian PAR bZip transcription factors results in epilepsy. *Genes Dev* **18:** 1397-1412.

Gachon F, Olela FF, Schaad O, Descombes P, and Schibler U (2006) The circadian PAR-domain basic leucine zipper transcription factors DBP, TEF, and HLF modulate basal and inducible xenobiotic detoxification. *Cell Metab* **4:** 25-36.

Gekakis N, Staknis D, Nguyen HB, Davis FC, Wilsbacher LD, King DP, Takahashi JS, and Weitz CJ (1998) Role of the CLOCK Protein in the Mammalian Circadian Mechanism. *Science* **280:** 1564-1569

Göttlicher M, Widmark E, Li Q, and Gustafsson JA (1992) Fatty acids activate a chimera of the clofibric acid-activated receptor and the glucocorticoid receptor. *Proc Natl Acad Sci U S A* **89:** 4653-4657.

Green CB, Takahashi JS, and Bass J (2008) The Meter of Metabolism. *Cell* **134:** 728-742.

Hrushesky WJ, Levi FA, Halberg F, and Kennedy BJ (1982) Circadian Stage Dependence of cis-Diamminedichloroplatinum Lethal Toxicity in Rats. *Cancer Res* **42:** 945-949.

Jin X, Shearman LP, Weaver DR, Zylka MJ, De Vries GJ, and Reppert SM (1999) A Molecular Mechanism Regulating Rhythmic Output from the Suprachiasmatic

Circadian Clock. *Cell* 96: 57-68.

Karbach U, Kricke J, Meyer-Wentrup F, Gorboulev V, Volk C, Loffing-Cueni D, Kaissling B, Bachmann S, and Koepsell H (2000) Localization of organic cation transporters OCT1 and OCT2 in rat kidney. *Am J Physiol Renal Physiol* **279:** F679-F687.

Katada S and Sassone-Corsi P (2010) The histone methyltransferase MLL1 permits the oscillation of circadian gene expression. *Nat Struct Mol Biol* **17:** 1414-1421.

Keller H, Dreyer C, Medin J, Mahfoudi A, Ozato K, and Wahli W (1993) Fatty acids and retinoids control lipid metabolism through activation of peroxisome proliferator-activated receptor-retinoid X receptor heterodimers. *Proc Natl Acad Sci U S A* **90:** 2160-2164.

Koyanagi S, Hamdan AM, Horiguchi M, Kusunose N, Okamoto A, Matsunaga N, and Ohdo S (2011) cAMP-response Element (CRE)-mediated Transcription by Activating Transcription Factor-4 (ATF4) Is Essential for Circadian Expression of the Period2 Gene. *J Biol Chem* **286:** 32416-32423.

Labrecque G and Bélanger PM (1991) Biological rhythms in the absorption, distribution, metabolism and excretion of drugs. *Pharmacol Ther* **52:** 95-107.

Lange RC, Spencer RP, and Harder HC (1972) Synthesis and distribution of a radiolabeled antitumor agent: cis-diamminedichloroplatinum (II). *J Nucl Med* **13:** 328-330.

Levi FA, Hrushesky WJ, Halberg F, Langevin TR, Haus E, and Kennedy BJ (1982a) Lethal nephrotoxicity and hematologic toxicity of cis-diamminedichloroplatinum

ameliorated by optimal circadian timing and hydration. *Eur J Cancer Clin Oncol* **18:** 471-477.

Levi FA, Hrushesky WJ, Blomquist CH, Lakatua DJ, Haus E, Halberg F, and Kennedy BJ (1982b) Reduction of cis-Diamminedichloroplatinum Nephrotoxicity in Rats by Optimal Circadian Drug Timing. *Cancer Res* **42:** 950-955.

Li S, Wu P, Yarlagadda P, Vadjunec NM, Proia AD, Harris RA, and Portilla D (2004) PPARα ligand protects during cisplatin-induced acute renal failure by preventing inhibition of renal FAO and PDC activity. *Am J Physiol Renal Physiol* **286:** F572–F580.

Li S, Gokden N, Okusa MD, Bhatt R, and Portilla D (2005) Anti-inflammatory effect of fibrate protects from cisplatin-induced ARF. *Am J Physiol Renal Physiol* **289:** F469–F480.

Litterst CL (1981) Alterations in the toxicity of cis-Dichlorodiammineplatinum-II and in tissue localization of platinum as a function of NaCl concentration in the vehicle of administration. *Toxicol Appl Pharmacol* **61:** 99-108.

Maemura K, de la Monte SM, Chin MT, Layne MD, Hsieh CM, Yet SF, Perrella MA, and Lee ME (2000) CLIF, a Novel Cycle-like Factor, Regulates the Circadian Oscillation of Plasminogen Activator Inhibitor-1 Gene Expression. *J Biol Chem* **275:** 36847-36851.

Martin G, Schoonjans K, Lefebvre AM, Staels B, and Auwerx J (1997) Coordinate Regulation of the Expression of the Fatty Acid Transport Protein and Acyl-CoA Synthetase Genes by PPARα and PPARγ Activators. *J Biol Chem* **272:** 28210-28217

Miller RP, Tadagavadi RK, Ramesh G, and Reeves WB (2010) Mechanisms of Cisplatin nephrotoxicity. *Toxins* **2:** 2490-2518.

Montero TD, Racordon D, Bravo L, Owen GI, Bronfman ML, and Leisewitz AV (2012) PPARα and PPARγ regulate the nucleoside transporter hENT1. *Biochem Biophys Res Commun* **419:** 405-411.

Morf J, Rey G, Schneider K, Stratmann M, Fujita J, Naef F, and Schibler U (2012) Cold-Inducible RNA-Binding Protein Modulates Circadian Gene Expression Posttranscriptionally. *Science* **338:** 379-383.

Nagothu KK, Bhatt R, Kaushal GP, and Portilla D (2005) Fibrate prevents cisplatin-induced proximal tubule cell death. *Kidney Int* **68:** 2680–2693.

Nakamura T, Yonezawa A, Hashimoto S, Katsura T, and Inui K (2010) Disruption of multidrug and toxin extrusion MATE1 potentiates cisplatin-induced nephrotoxicity. *Biochem Pharmacol* **80:** 1762-1767.

Ohdo S (2007) Chronopharmacology Focused on Biological Clock. *Drug Metab Pharmacokinet* **22:** 3-14.

Ohdo S (2010) Chronotherapeutic strategy: Rhythm monitoring, manipulation and disruption. *Adv Drug Deliv Rev* **62:** 859-875.

Oishi K, Shirai H, and Ishida N (2005) CLOCK is involved in the circadian transactivation of peroxisome-proliferator-activated receptor α (PPARα) in mice. *Biochem J* **386:** 575-581.

Oishi K, Uchida D, Ishida N (2008) Circadian expression of FGF21 is induced by PPARa activation in the mouse liver. *FEBS Lett* **582:** 3639-3642.

Otsuka M, Matsumoto T, Morimoto R, Arioka S, Omote H, and Moriyama Y (2005) A human transporter protein that mediates the final excretion step for toxic organic cations. *Proc Natl Acad Sci U S A* **102:** 17923-17928.

Pabla N and Dong Z (2008) Cisplatin nephrotoxicity: mechanisms and renoprotective strategies. *Kidney Int* **73:** 994-1007.

Preitner N, Damiola F, Molina LM, Zakany J, Duboule D, Albrecht U, and Schibler U (2002) The orphan nuclear receptor REV-ERBalpha controls circadian transcription within the positive limb of the mammalian circadian oscillator. *Cell* **110:** 251-260.

Qi Z, Whitt I, Mehta A, Jin J, Zhao M, Harris RC, Fogo AB, and Breyer MD (2004) Serial determination of glomerular filtration rate in conscious mice using FITC-inulin clearance. *Am J Physiol Renal Physiol* **286:** F590-F596.

Siddik ZH, Newell DR, Boxall FE, and Harrap KR (1987) The comparative pharmacokinetics of carboplatin and cisplatin in mice and rats. *Biochem Pharmacol* **36:** 1925-1932.

Terada T and Inui KI (2007) Gene expression and regulation of drug transporters in the intestine and kidney. *Biochem Pharmacol* **73:** 440-449.

Urakami Y, Okuda M, Masuda S, Saito H, and Inui KI (1998) Functional Characteristics and Membrane Localization of Rat Multispecific Organic Cation Transporters, OCT1 and OCT2, Mediating Tubular Secretion of Cationic Drugs. *J Pharmacol Exp Ther* **287:** 800-805.

Yonezawa A, Masuda S, Yokoo S, Katsura T, and Inui K (2006) Cisplatin and Oxaliplatin, but Not Carboplatin and Nedaplatin, Are Substrates for Human Organic Cation

Transporters (SLC22A1–3 and Multidrug and Toxin Extrusion Family). *J Pharmacol Exp Ther* **319:** 879-886.

Molecular Pharmacology Fast Forward. Published on February 24, 2014 as DOI: 10.1124/mol.113.089805
This article has not been copyedited and formatted. The final version may differ from this version.

Footnotes

This work was supported by Grant-in-Aid for Scientific Research on Innovative Areas [25136716 to S.O.] and Grant-in-Aid for Scientific Research (B) [24390149 to S.K.] from Japan Society for the Promotion of Science

Molecular Pharmacology Fast Forward. Published on February 24, 2014 as DOI: 10.1124/mol.113.089805
This article has not been copyedited and formatted. The final version may differ from this version.

Figure legends

Fig. 1. Dosing-time dependency of CDDP-induced nephrotoxicity in mice. Wild-type (A) or *Clock* mutant (*Clock/Clock*) mice (B) were injected intravenously with a single dosage of CDDP (15 mg/kg) or equivalent volume of saline at the indicated times. Blood samples were collected 72 h after the CDDP injection. Blood urea nitrogen (BUN) levels in the serum were assessed as an index of CDDP-induced nephrotoxicity. Each value is the mean ± S.E. (n = 3-6). *, $P < 0.05$, significant difference between the groups.

Fig. 2. Dosing-time dependent changes in CDDP pharmacokinetics in mice. (A) Dosing-time dependent differences in the area under the serum Pt concentration-time curve from 1 to 4 h (AUC_{1-4}) after the CDDP injection (15 mg/kg, i.v.) in wild-type or *Clock* mutant (*Clock/Clock*) mice. (B) Dosing-time dependent differences in the renal clearance (CLr) of CDDP (15 mg/kg, i.v.) in wild-type or *Clock/Clock* mice. (C) Dosing-time dependent differences in the amount of Pt incorporated into the renal DNA of wild-type or *Clock/Clock* mice at 4 h after the CDDP (15 mg/kg, i.v.) injection. (D) Time-dependent changes in the glomerular filtration rate (GFR) in wild-type or *Clock/Clock* mice. Each value is the mean ± S.E. (n = 5-16). **, $P < 0.01$; *, $P < 0.05$, significant difference between the groups.

Fig. 3. Influence of the *Clock* gene mutation on the expression of OCT2/*Slc22a2* and MATE1/*Slc47a1* in the kidneys of mice. (A) Temporal expression profiles of the OCT2 and MATE1 protein in the renal membrane fraction of the kidneys of wild-type or *Clock*

Molecular Pharmacology Fast Forward. Published on February 24, 2014 as DOI: 10.1124/mol.113.089805
This article has not been copyedited and formatted. The final version may differ from this version.

mutant (*Clock/Clock*) mice. (B) Temporal mRNA expression profiles of *Slc22a2* and *Slc47a1* gene in the kidneys of wild-type or *Clock/Clock* mice. Significant 24-h variations in *Slc22a2* mRNA ($P < 0.01$, ANOVA) were observed in the kidneys of wild-type mice. Each point is the mean ± S.E. (n = 3-6). **, $P < 0.01$; *, $P < 0.05$, significantly different from wild-type mice at the corresponding times.

Fig. 4. Transcriptional regulation of *Slc22a2* by PPARα. (A) Location of consensus sequences for response element to circadian transcriptional factors within the mouse *Slc22a2* promoter region. Closed boxes indicate the sites that matched the PPAR response elements (PPREs), retinoic acid–related orphan nuclear receptor response elements (ROREs), or cAMP binding protein (CREB) response elements (CREs). The number of nucleotide residues indicates the distance from the transcription start site. (B) The ability of PPARα/RXRα, RORα, or ATF4 to induce transactivation of the luciferase reporter construct *Slc22a2* (-2,101)-Luc or pGL4.12 empty reporter. Luciferase activities were assayed 24 h after transfection. (C) Cells were transfected with luciferase reporter constructs containing various lengths of the promoter region of the mouse *Slc22a2* gene in the absence or presence of PPARα and RXRα expression vectors. Each value represents the mean ± S.E. of 3 experiments.

Fig. 5. CLOCK rhythmically drives the renal expression of *Slc22a2*/OCT2 through the mediation of PPARα. (A) Temporal expression profiles of PPARα and RXRα in nuclear fractions of the kidneys of wild-type or *Clock* mutant (*Clock/Clock*) mice. The

Molecular Pharmacology Fast Forward. Published on February 24, 2014 as DOI: 10.1124/mol.113.089805
This article has not been copyedited and formatted. The final version may differ from this version.

TATA-binding protein (TBP) indicates the approximately equal loading of nuclear extracts. (B) Temporal profiles of PPARα binding to the promoter region of the mouse *Slc22a2* gene in the kidneys of wild-type or *Clock/Clock* mice. (C) Temporal expression profile of *Slc22a2* mRNA in the kidneys of wild-type or PPARα-null mice. (D) Dosing-time dependent differences in the renal clearance (CLr) of CDDP (15 mg/kg, i.v.) in wild-type or PPARα-null mice. (E) Dosing-time dependent differences in the amount of Pt incorporated into the renal DNA of wild-type or PPARα-null mice at 4 h after the CDDP (15 mg/kg, i.v.) injection. Each value is the mean ± S.E. (n = 4-6). **, $P < 0.01$; *, $P < 0.05$, significant difference between the groups.

Fig. 6. Schematic representation of the mechanism for dosing-time dependent changes in CDDP-induced nephrotoxicity in mice. In wild-type mice, the amount of glomerular filtrated CDDP is increased during the dark phase resulting in the enhancement of its renal clearance. However, during this time windows, the renal expression of OCT2 is low level, so that incorporation of CDDP into renal cells is decreased by injecting the drug during the dark phase. Therefore, the nephrotoxic effect of CDDP is attenuated by injecting the drug at the times of day when renal expression of OCT2 is decreased. In *Clock* mutant (*Clock/Clock*) mice, the renal clearance of CDDP remains at low level throughout the day. Neither OCT2 nor MATE1 exhibit circadian oscillation in the kidneys of Clock/Clock mice. The expression levels of those transporters are decreased in Clock/Clock mice. Consequently, CDDP is likely accumulated in renal cells after the injection of the drug at both light and dark phases. This may account for severe nephrotoxic effect of CDDP in

Molecular Pharmacology Fast Forward. Published on February 24, 2014 as DOI: 10.1124/mol.113.089805
This article has not been copyedited and formatted. The final version may differ from this version.

Clock/Clock mice regardless of its dosing time.

Fig. 7. Kinetic analysis of CDDP accumulation in renal cells. (A) Schematic model to describe the time profile of Pt accumulation in renal cells. The influx rate constant (k_{in}), efflux rate constant (k_{out}), Pt concentration (*Ct*), and volume of cells (*Vc*) are indicated. (B) Validation analysis of the predicted intracellular concentration–time profiles of Pt following the administration of CDDP. (C) The prediction of dosing time-dependent differences in the intracellular concentration–time profiles of Pt following the administration of CDDP in wild-type and *Clock* mutant (*Clock/Clock*) mice. Values of k_{in} and k_{out} are defined based on the mean value of the protein band intensities of OCT2 and MATE1, respectively.

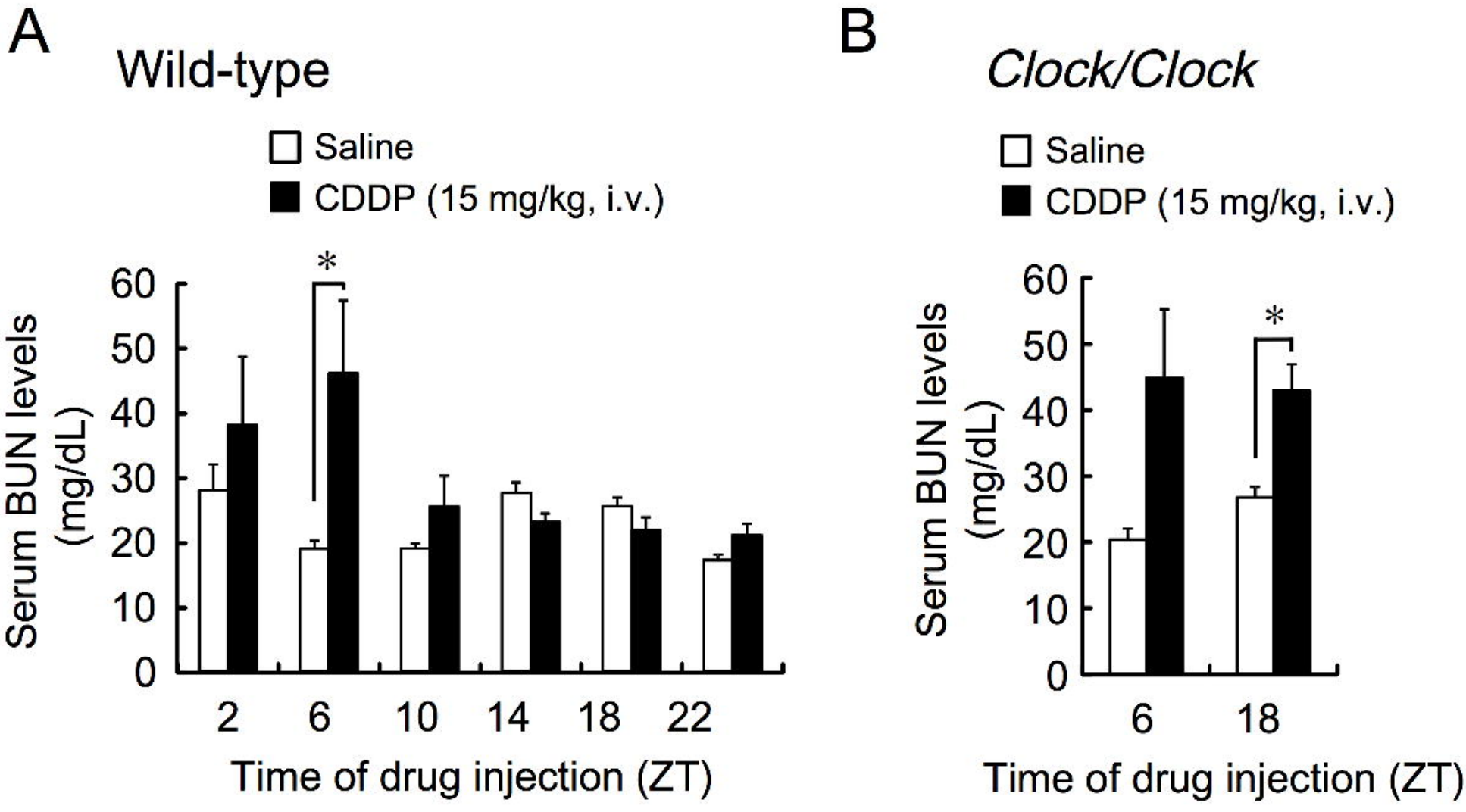
A
Wild-type
Saline
CDDP (15 mg/kg, i.v.)
Serum BUN levels (mg/dL)
60
50
40
30
20
10
0
*
2
6
10
14
18
22
Time of drug injection (ZT)
B
Clock/Clock
Saline
CDDP (15 mg/kg, i.v.)
Serum BUN levels (mg/dL)
60
50
40
30
20
10
0
*
6
18
Time of drug injection (ZT)

Figure 1

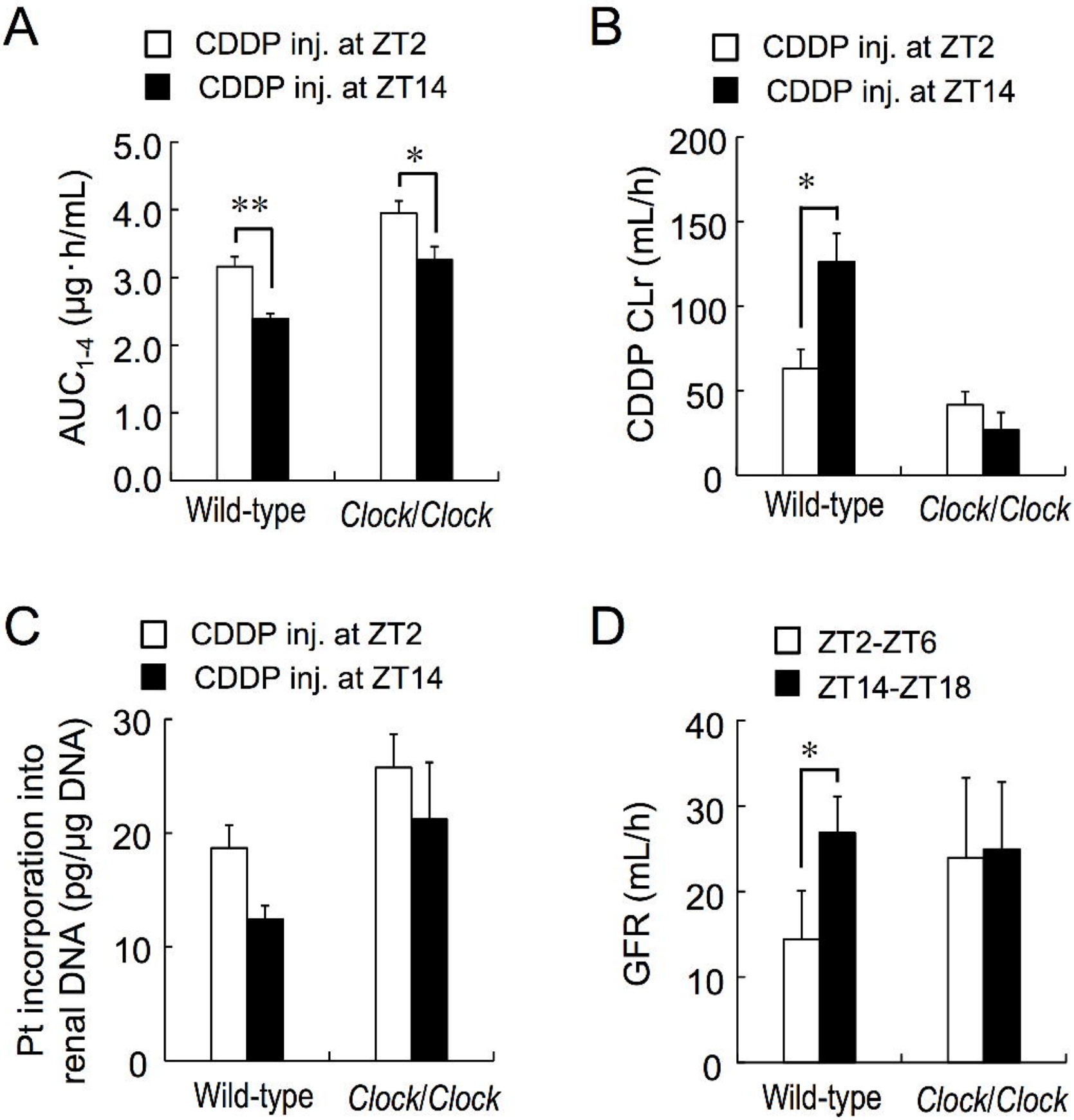
A
CDDP inj. at ZT2
CDDP inj. at ZT14
AUC1-4 (μg·h/mL)
5.0
4.0
3.0
2.0
1.0
0.0
**
*
Wild-type
Clock/Clock
B
CDDP inj. at ZT2
CDDP inj. at ZT14
CDDP CLr (mL/h)
200
150
100
50
0
*
Wild-type
Clock/Clock
C
CDDP inj. at ZT2
CDDP inj. at ZT14
Pt incorporation into renal DNA (pg/μg DNA)
30
20
10
0
Wild-type
Clock/Clock
D
ZT2-ZT6
ZT14-ZT18
GFR (mL/h)
40
30
20
10
0
*
Wild-type
Clock/Clock

Figure 2

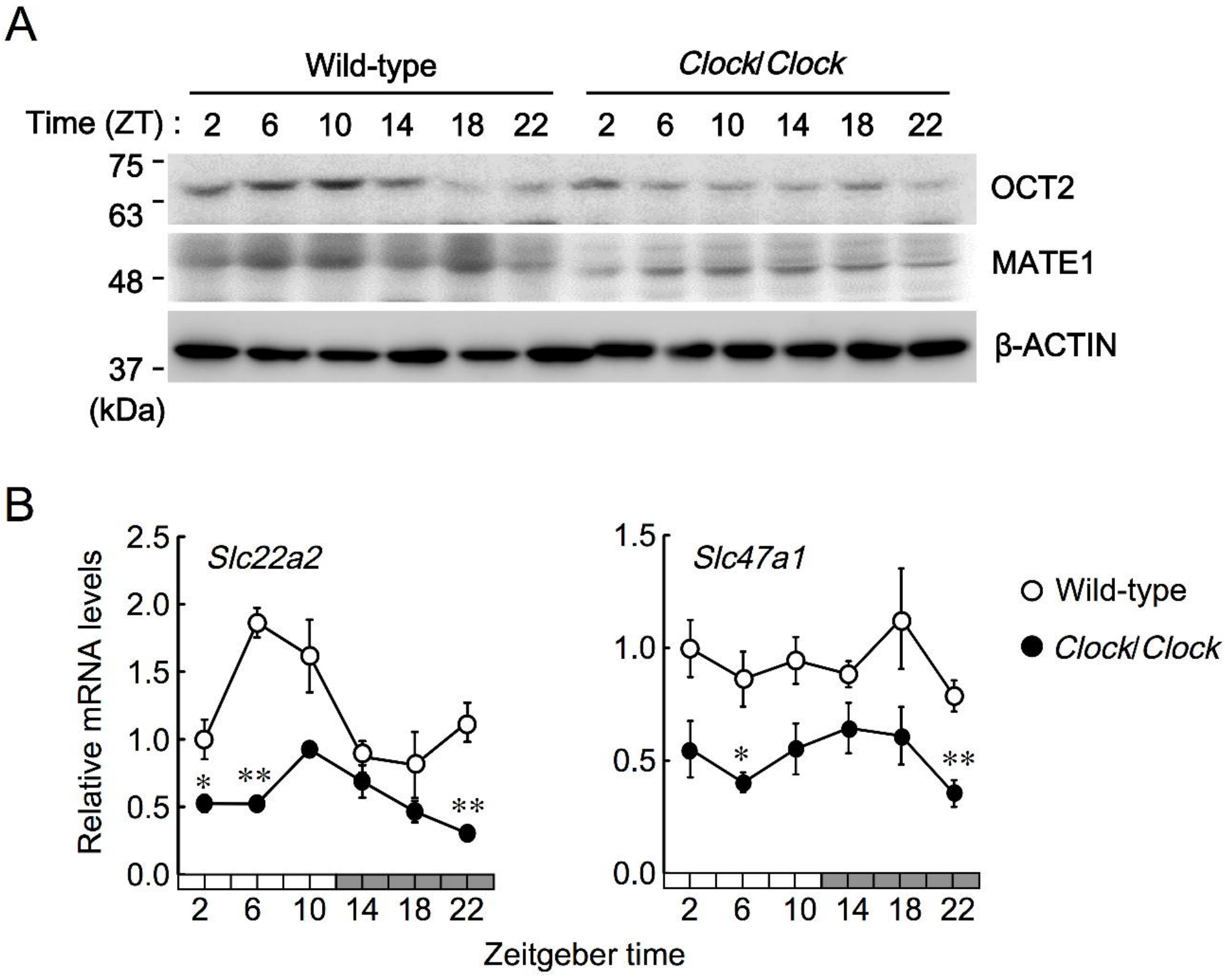
A
Wild-type
Clock/Clock
Time (ZT) : 2 6 10 14 18 22 2 6 10 14 18 22
75
63
48
37
(kDa)
OCT2
MATE1
β-ACTIN
B
Slc22a2
Slc47a1
Relative mRNA levels
2.5
2.0
1.5
1.0
0.5
0.0
1.5
1.0
0.5
0.0
*
**
**
*
**
2 6 10 14 18 22
2 6 10 14 18 22
Zeitgeber time
Wild-type
Clock/Clock

Figure 3

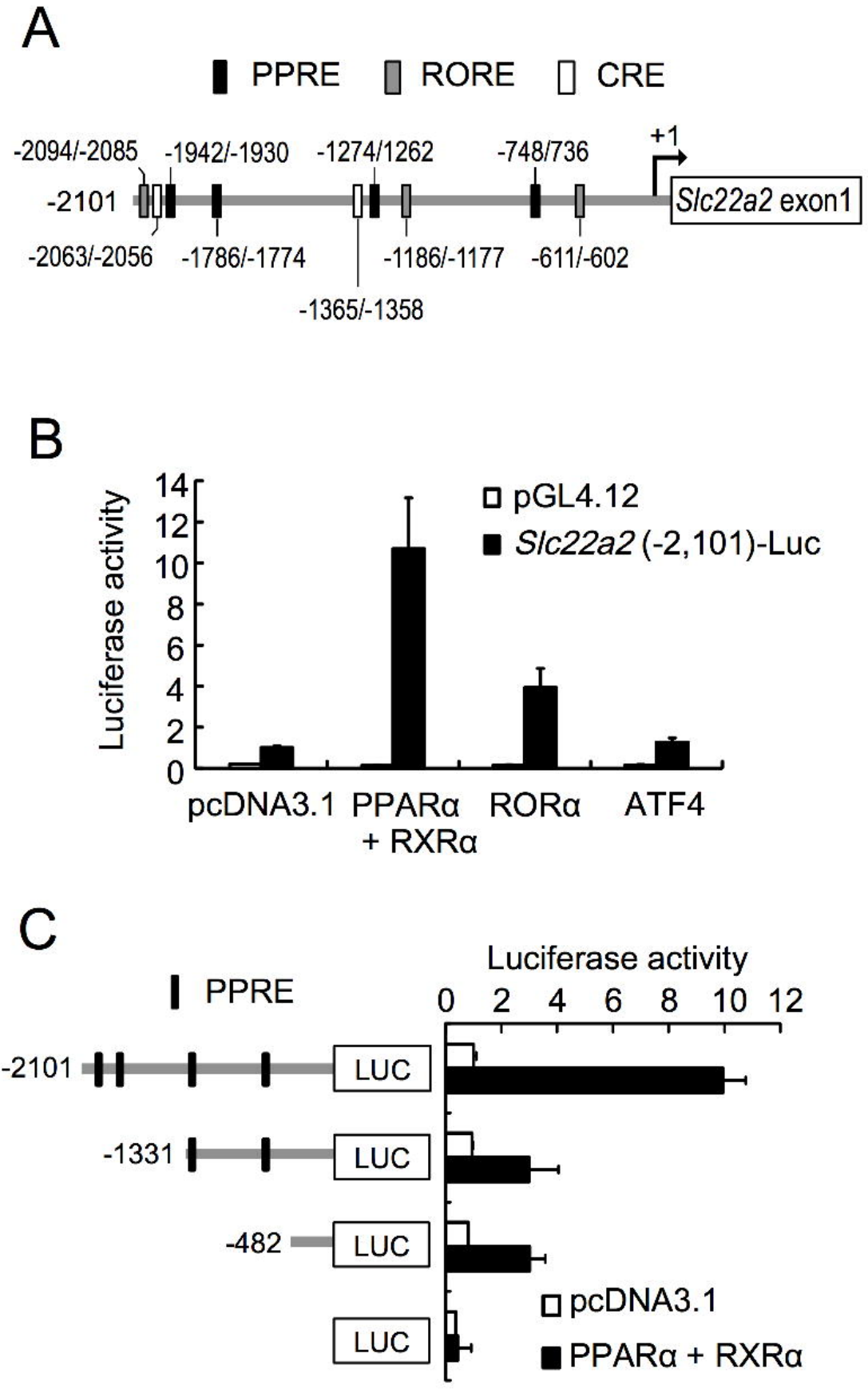
A
PPRE
RORE
CRE
-2094/-2085
-1942/-1930
-1274/1262
-748/736
+1
-2101
Slc22a2 exon1
-2063/-2056
-1786/-1774
-1186/-1177
-611/-602
-1365/-1358
B
Luciferase activity
14
12
10
8
6
4
2
0
pGL4.12
Slc22a2 (-2,101)-Luc
pcDNA3.1
PPARα + RXRα
RORα
ATF4
C
PPRE
Luciferase activity
0 2 4 6 8 10 12
-2101
-1331
-482
LUC
LUC
LUC
LUC
pcDNA3.1
PPARα + RXRα

Figure 4

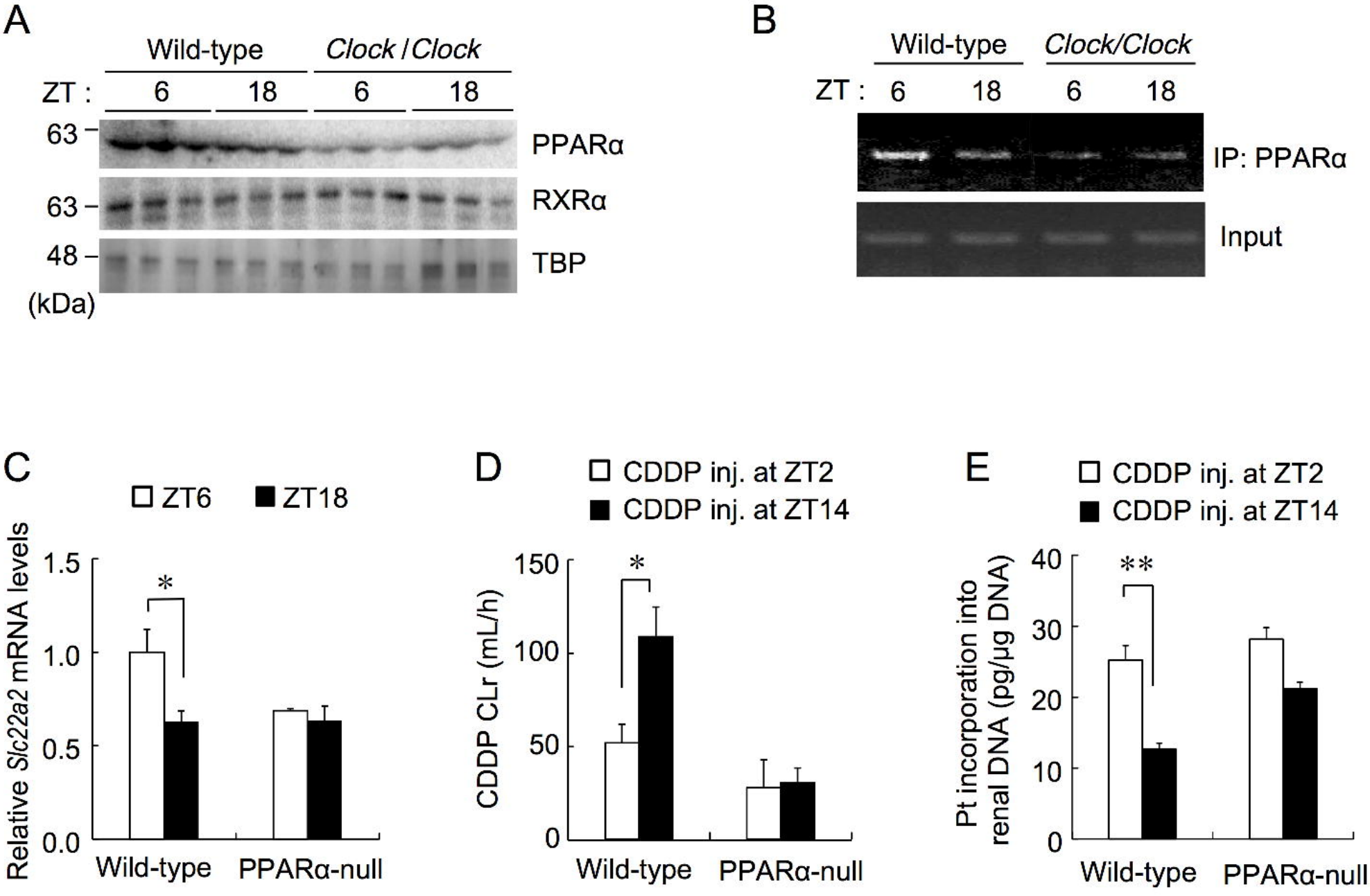
A
Wild-type
Clock / Clock
ZT :
6
18
6
18
63
PPARα
63
RXRα
48
TBP
(kDa)
B
Wild-type
Clock/Clock
ZT :
6
18
6
18
IP: PPARα
Input
C
ZT6
ZT18
Relative Slc22a2 mRNA levels
1.5
1.0
0.5
0.0
*
Wild-type
PPARα-null
D
CDDP inj. at ZT2
CDDP inj. at ZT14
CDDP CLr (mL/h)
150
100
50
0
*
Wild-type
PPARα-null
E
CDDP inj. at ZT2
CDDP inj. at ZT14
Pt incorporation into renal DNA (pg/μg DNA)
40
30
20
10
0
**
Wild-type
PPARα-null

Figure 5

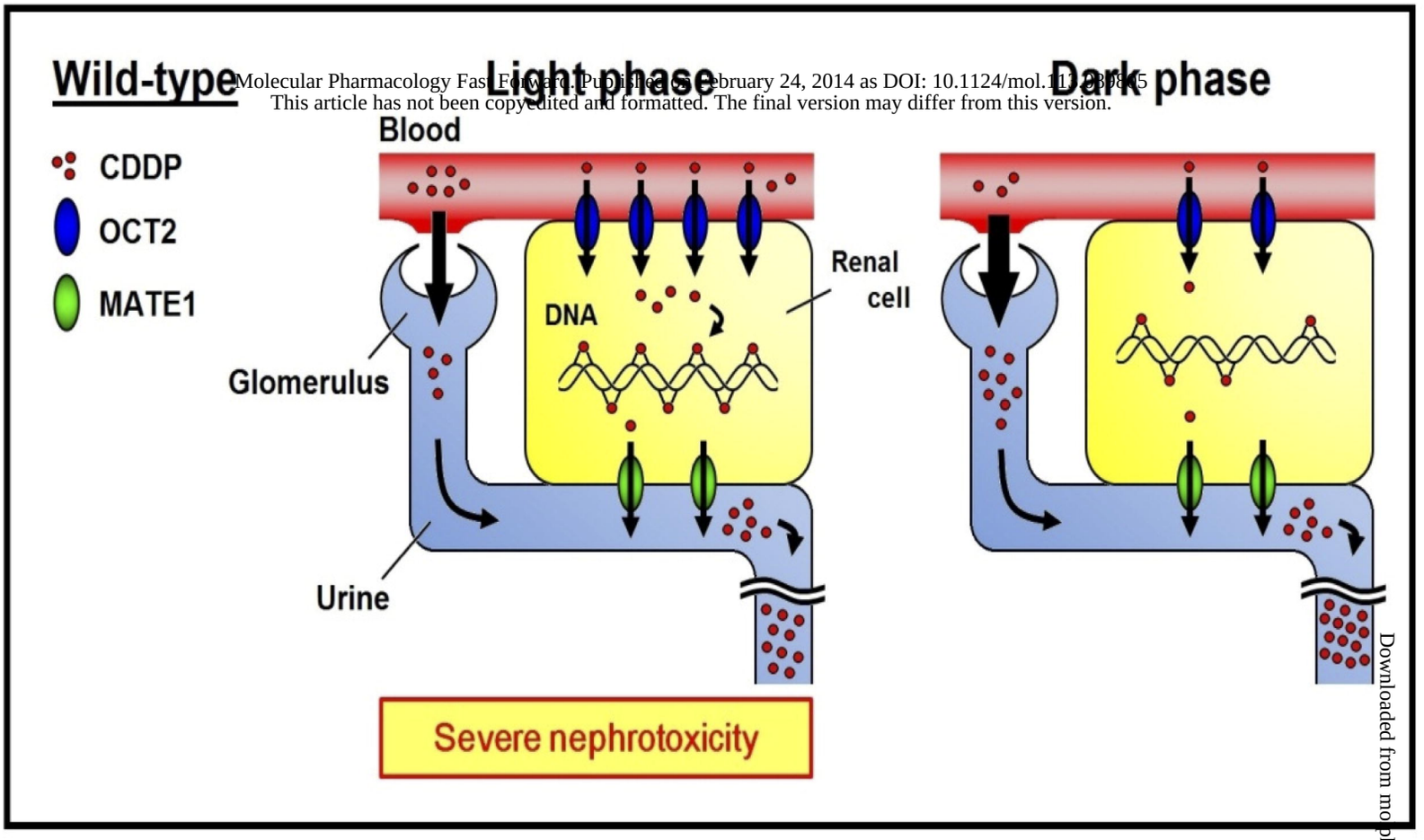

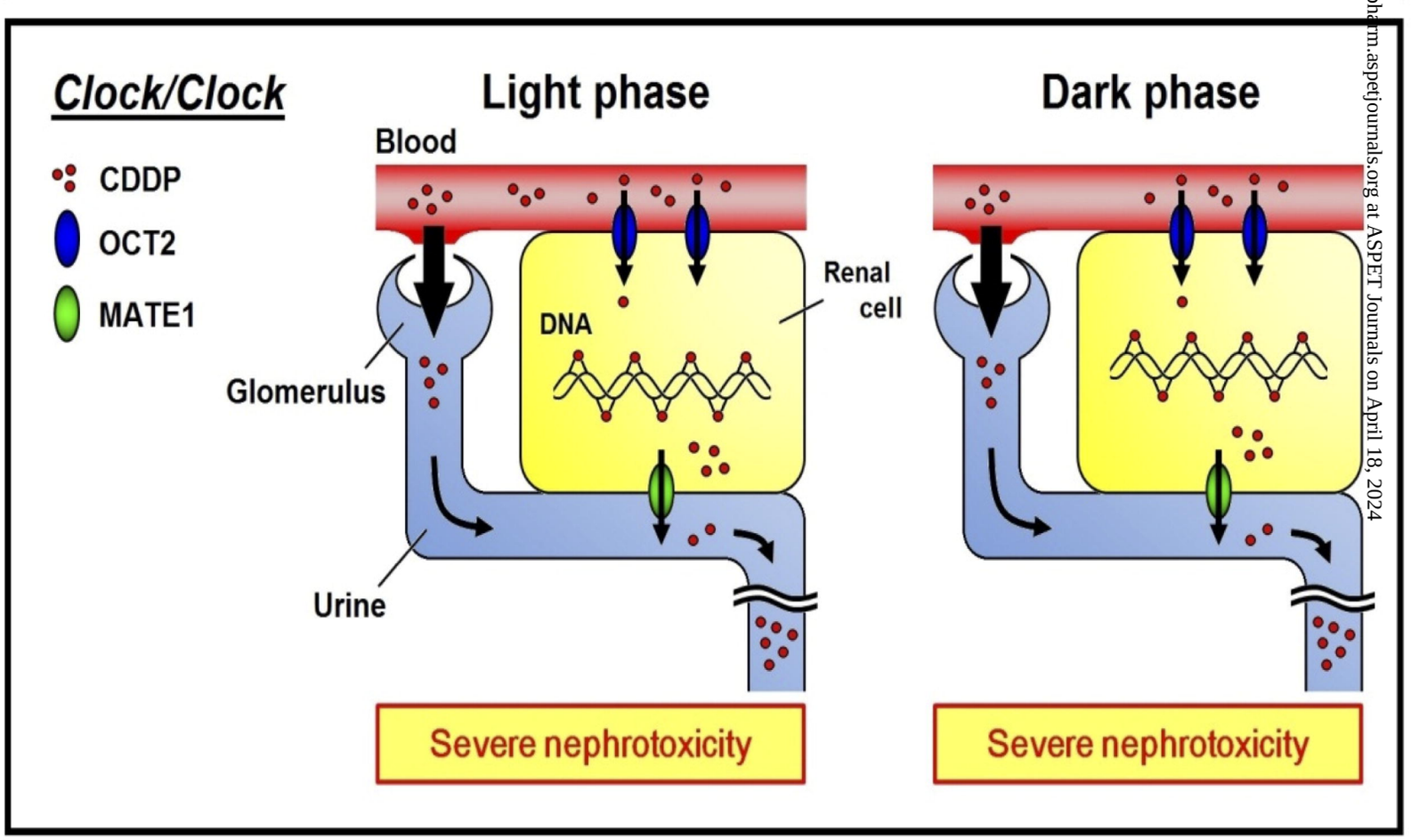

Figure6

A

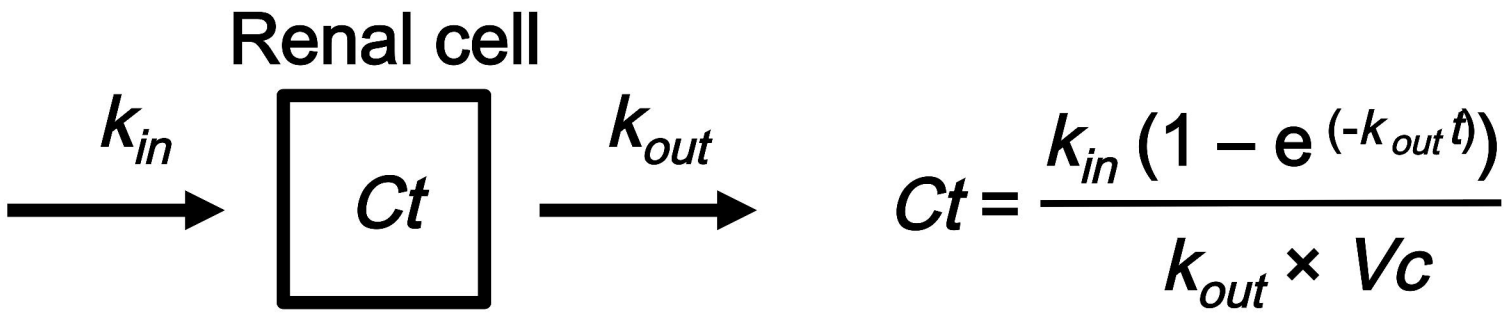

B

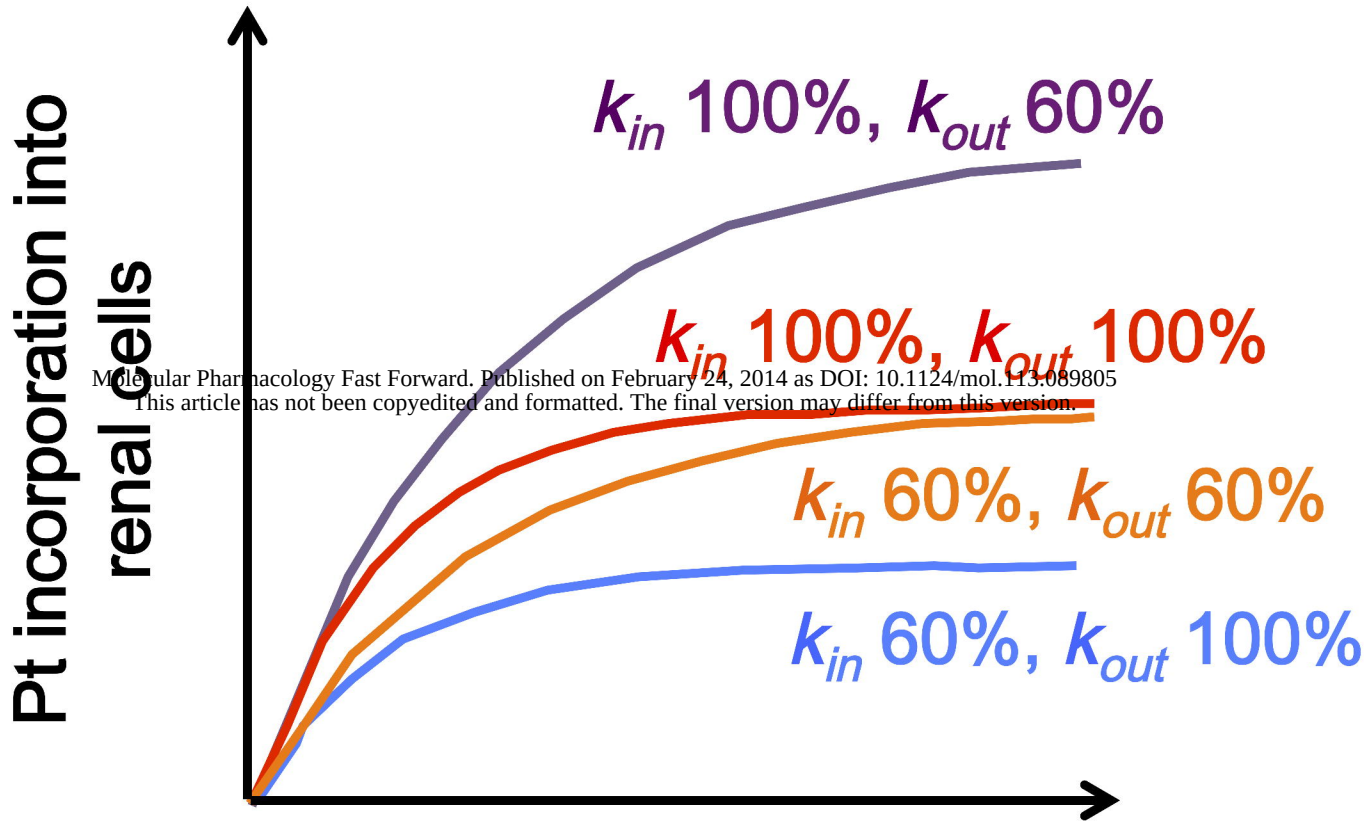

Molecular Pharmacology Fast Forward. Published on February 24, 2014 as DOI: 10.1124/mol.113.089805
This article has not been copyedited and formatted. The final version may differ from this version.

Time after CDDP injection

C

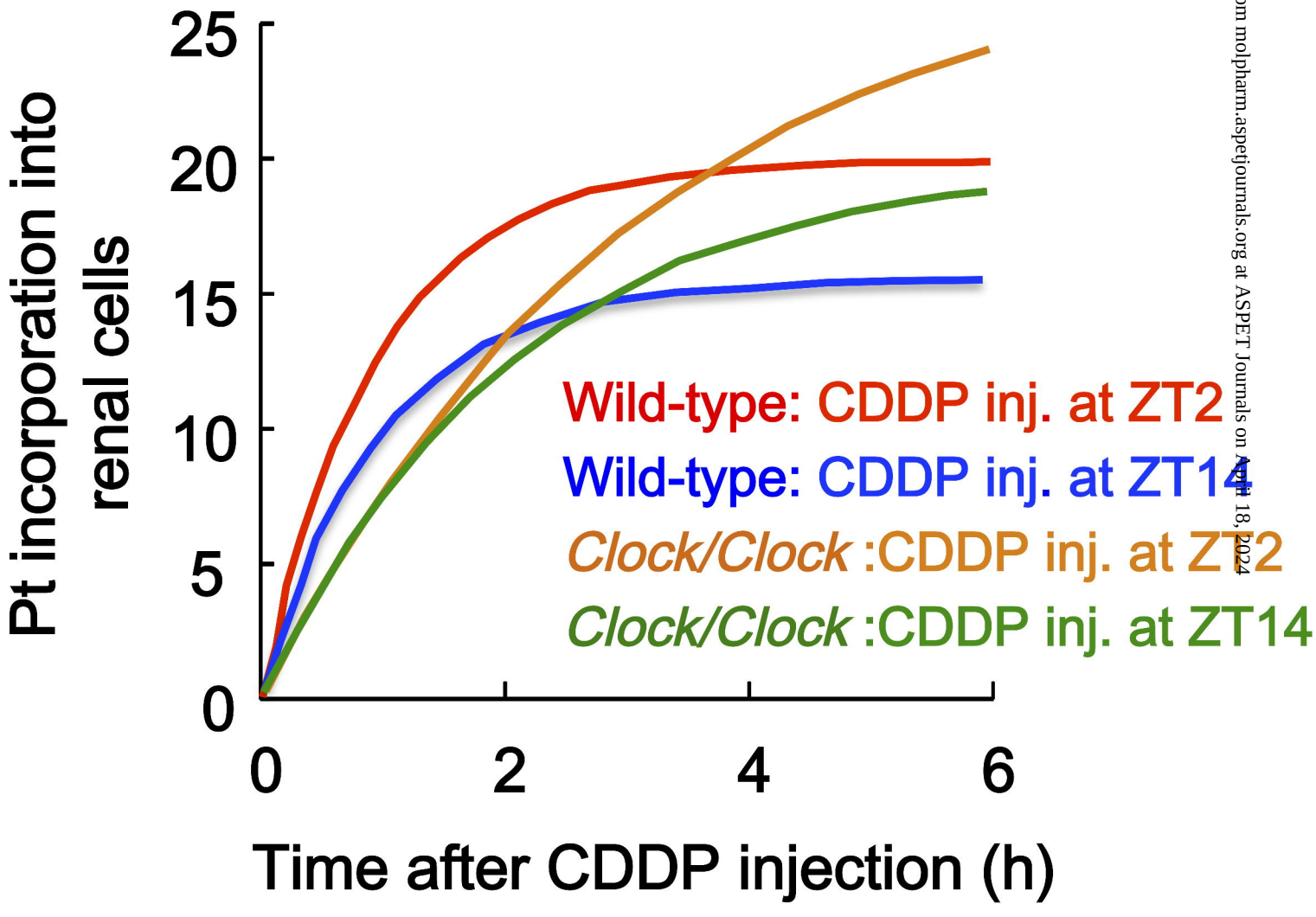

Figure 7